

Electrochemical Analysis of Ki67 Protein As Pancreatic Cancer Biomarker Based on Graphene-Polydopamine Nanocomposite

Liguo Hao^{1,2*}, Lijie Liu³, Xin Meng⁴, Hongsheng Cui⁴, Zixu Wang¹

¹ 1. Medical Technology School of Qiqihar Medical University, No. 333 Bukui North Road, Jianhua District, Qiqihar City, Heilongjiang Province 161006, P.R. China

² Academy of Medical Sciences of Qiqihar, No. 333 Bukui North Road, Jianhua District, Qiqihar City, Heilongjiang Province 161006, P.R. China

³ College of Life Science and Agriculture Forestry, Qiqihar University, Qiqihar City, Heilongjiang Province 161006, P.R. China

⁴ Third Affiliated Hospital of Qiqihar Medical University, Qiqihar City, Heilongjiang Province 161006, P.R. China

*E-mail: 363046903@qq.com

Received: 24 January 2017 / Accepted: 3 March 2017 / Published: 12 March 2017

An electrochemical immunosensor was studied for sensitive detection of Ki-67 protein based on a dual amplification mechanism resulting from Au nanoparticles (AuNP)–polydopamine (PDA) as the sensor platform. By utilizing PDA, biomolecules were immobilized for both the construction of the sensor platform and the signal labeling. The particular platform of AuNP-PDA, as well as synthesizing horseradish peroxidase (HRP)-antibody (Ab2) functionalized AuNP-PDA@graphene was utilized to immensely enhance the sensitivity. The amperometry determination was used to obtain a linear response range of Ki-67 which was from 4 to 800 pg/mL, along with a very low detection limit (1.7 pg/mL)

Keywords: Pancreatic neuroendocrine tumor; Ki-67; Immunosensor; Polydopamine; Graphene

1. INTRODUCTION

In terms of pancreatic neuroendocrine tumor (PNET), of which the biological behavior is generally unpredictable, the most significant prognostic factor for it is probably tumor cell proliferation. Substantially, both mitoses and/or the Ki-67 index, as the basis of the nearest 2010 WHO grading system for gastrointestinal and pancreatic neuroendocrine tumors [1], have been included in all grading systems for PNET [2-5]. The Ki-67 index, which has been applied more frequently as a

requisite constituent of pathology reports for all neuroendocrine tumors [6], specifically, is quite helpful in small biopsy specimens or for metastases where it is unlikely for a more sizeable removed portion of the tumor to become useful. Nevertheless, by now, the most appropriate method of quantitating immunohistochemical staining for the Ki-67 index is still far more concluded by any consensus of pathologists, who usually determine the Ki-67 index including eyeball estimation (EE) of the percentage of positive cells, manual counting (MC), or automated digital imaging analysis (DIA), via three methods. Concerning EE, high inter- and intra-observer variability was anticipated before, but it is particularly hard, between times, when the Ki-67 index falls between 1 and 3 % as the 2010 WHO classification system is adopted; concerning MC, for common pathology practice, it was too time-wasting particularly when 2000 cells was counted by certain systems [7]. It was demonstrated by the Delphic consensus, that the proportion of who felt MC should not be successfully done was 75 %; concerning DIA, what was also agreed by the Delphic consensus was that, although it was impressive and quite useful at lots of institutions, DIA could not be completely effective for regular practice, and the proportion of who considered that DIA had not been already available for general operation was 63 %. A comparison for the four approaches including EE, DIA, and eye-counting-used manual counting either on a camera-captured/printed image or under a microscope, was made in a recent study [8], and the conclusion made by the authors was that, the most trustworthy method with the highest reproducibility, was manual counting using a camera-captured or printed image. Finally, the Delphic consensus consented that, subjecting to the shortage of data regarding intra- and interobserver reproducibility, comparison with the mitotic rate to predict the clinical diagnosis, association of automated quantification with the clinical diagnosis, and estimate of intratumoral heterogeneity, there were some controversies for the usage of the Ki-67 index for NETs. Consequently, obtaining a direct method that is not complicated for Ki67 determination has been a key factor in the field of clinical medicine.

Biosensing is critical for improving the standards of human life quality. Based on biosensors and biosensing protocols, it's possible to sensitively and selectively detect a broad range of compounds with health care for point-of-care analyses of diseases, security applications, and environmental safety. Graphene, a type of one-atom-thick material, is constitutive of sp^2 -bonded carbon with a honeycomb structure. A large polyaromatic molecule of semi-infinite size is resembled by it [9]. Nanomaterials based on graphene have attracted a vast range of attention in the last five years. Single-layer graphene sheets have some fascinating characteristics, e.g. high mechanical strength [10], high thermal and elasticity conductivity, tunable optical properties [11], a tunable band gap, demonstration of the room temperature quantum Hall effect, and very high room-temperature electron mobility. Similarly, but not identical interesting characteristics are demonstrated by few-, double-, and multilayer graphene. And the scientific community, particularly in the fields of physics, chemistry, and materials, is very excited by these properties. Graphene, with low environmental impact and low cost as a conductive yet transparent material, is an ideally perfect material for biosensor-based devices and the construction of sensors in miscellaneous transduction modes. In that graphene (GR) has fast electron transportation and high biocompatibility, GR-based composites, as electrode materials, are fascinating for the development of enhanced label-free immunosensors. It was reported by a few groups that the

development of ultra-high-sensitive electrochemical biosensors can be efficiently enhanced by GR [12-17].

The deficiency of neurotransmitter, which is dopamine (2-(3,4-dihydroxyphenyl)ethylamine) as everyone knows, results in Parkinson's disease [18]. Both alkylamine (yellow, lysine-like) and catechol (blue, dopamine-like) functionalities constitute the structure of Dopamine. Polydopamine (PDA), a polymeric precipitate, is what Dopamine change into under the circumstances of neutral solution with air. In addition, with all sorts of organic and inorganic materials, the PDA film can be modified and the resultant surface will undergo more reaction, widening the range of applications [19]. For instance, Wang and partners put forward a selective electrochemical sensor with high sensitivity based on polydopamine/ multiwalled carbon nanotubes/gold nanoparticles composites [20], and a new electrode was made by electrodeposition of gold nanoparticles (Au NPs). Besides, Li and partners put forward that on overoxidized PDA modified gold electrode [21]

The purpose of this study is to develop a high-efficient PDA-based electrochemical immunoassay for detecting Ki67 in clinical diagnosis. For sensitive detection of Ki67, an electrochemical immunosensor has been studied in this paper, based on a dual amplification mechanism originating from the multienzyme-antibody functionalized AuNP-PDA@graphene and the AuNP-PDA sensor platform. Through loading a mass of biomolecules, immensely extended sensitivity was achieved. Due to the catalytic reaction between the carried HRP and the H_2O_2 -*O*-phenylenediamine (OPD) system, the electrochemical signal of the captured PDA@graphene-AuNP and carried HRP-anti-Ki67 are achievable and can be obtained quickly and sufficiently. Potential applications in the screening of rabbit tumor of pancreatic cancer have been demonstrated by the immunosensor proposed in this report.

2. EXPERIMENTS

2.1. Chemicals

We purchased Ki67 antigen and Ki67 antibody from Shenzheng Biotech CO., LTD. Silver nitrate (AgNO_3), Chloroauric acid (HAuCl_4) and hexachloropalladic(IV) acid (H_2PdCl_6) were bought from Shanghai Chemical Reagent Co. (Shanghai, China). Dopamine and lyophilized bovine serum albumin (BSA) (99%) were bought from Sigma-Aldrich. Phosphate buffer saline (PBS, 10 mM, pH 7.4) was provided by Na_2HPO_4 and KH_2PO_4 . Graphene oxide (GO) was got from graphite powder via a modified Hummers approach. The standard Ki67 antigen solution was prepared in the PBS and stored at 4 °C. We fabricated all of aqueous solutions using ultrapure water (Milli-Q, Millipore). And all of other chemicals were used as received and of analytical grade.

2.2. Apparatus

Using 1.0 M KCl as the supporting electrolyte, electrochemical impedance spectroscopy (EIS) was implemented together with an Autolab electrochemical analyzer (Eco Chemie, The Netherlands)

in a 10 mM $K_3Fe(CN)_6/K_4Fe(CN)_6$ (1:1) mixture, via the adoption of an alternating current voltage of 5.0 mV, and the frequency range was 0.1 Hz–10 kHz. A CHI 760 electrochemical workstation was adopted.

2.3. Preparation of HRP-Ab₂-AuNP-PDA@graphene Bioconjugate

Tentatively, we added 100 mg graphene, 200 mg dopamine, and 120 mg Tris which were diluted via 1 min of sonication in ice-water bath, into 100 mL deionized water, and the aquired mixture was operated by a magnetic agitation at a room temperature of 20 °C for 36 h. After the filtering and washing of the coated graphene (PDA@graphene), 25 mg was diffused into $HAuCl_4$ aqueous solution (25 mL, 1.4 mM). At room temperature for 2 h, the mixture was gently agitated, then filtrated and washed, making it split to AuNP-PDA@graphene. The fabrication procedure of the HRP-Ab₂-AuNP-PDA@graphene bioconjugate was as follows. Firstly we added one milligram of AuNP-PDA@graphene in 2 mL pH 7 PBS. This mixture was mildly mixed with 150 μ L of Ab₂ at 2.0 μ g/mL and 300 μ L of HRP at 1.0 mg/mL, and then blocked by 100 μ L of 1% BSA solution. Subsequently, we washed the oiled drop after centrifugation with the use of a buffer of pH 7 PBS, 0.05% Tween (PBST).

2.4. Antibody Immobilization

Directly, we made 0.50 mg/mL dopamine dissolved in 10 mM pH 8.5 Tris–HCl, and sanitized ITO glasses with acetone and ethanol, and then dipped into the solution for 12 h after cleaning the coated surfaces with water and drying them by N_2 gas to get PDA/ITO. Then for absorbing the secondary modifier AuNP, we utilized PDA as the substrate, while for getting AuNP-PDA/ITO, we immersed PDA/ITO into the AuNP for 12 h. Next was immobilizing Ab₁ onto the AuNP-PDA/ITO, and laying out twenty microliters of 0.10 mg/mL anti-Ki67 antibody solution (50 mM pH 7 PBS) onto the AuNP-PDA/ITO surface. After incubation for more than 15 h, we rinsed them with PBST to make absorbed Ab₁ physically removed. We used 1% BSA solution to block the electrodes for 1 h under a room temperature, and cleaned the electrodes with PBST. After aspiration was incubating Ab₁ modified electrodes for 1 h at 37 °C, with 10 μ L of detecting Ag samples. When the reaction of binding between Ab₁ and Ag finished, we immersed the electrodes into the 10 μ L HRP-Ab₂, HRP-Ab₂-AuNP-PDA@graphene or other labeled HRP-Ab₂ bioconjugate solution, for 50 min as the time of incubation. At last, considering that a background response before measurement could be caused by bound conjugations, we completely washed these electrodes with PBST to nonspecifically get rid of bound conjugations.

2.5. Rabbit tumor model

All studies of the animal were operated complying with the protocol consented and surveilled by the Washington University Animal Studies Committee. We anesthetized Male New Zealand White

rabbits (~ 2 kg) using intramuscular xylazine and ketamine. Experimental protocols, as well as all procedures of animal care, were directed and consented in conformity to guidelines of Washington University.

3. RESULTS AND DISCUSSION

FTIR (Figure 1A) characterized the cleaned PDA@graphene. The spectrum of GO displays peaks at 1710, 1592, 1398 and 1024 cm^{-1} , which belong to the C=O stretching of COOH groups, C=C vibrations, C—OH stretching vibrations and C—O vibrations from alkoxy groups, respectively.[22-24]. While PDA presents only several features of intense absorption: around 1605 cm^{-1} from aromatic rings and around 3421 cm^{-1} from catechol —OH groups, lots of narrow peaks and a feature of small molecules were demonstrated by Dopamine. At the same positions, weak absorption was given by the pure graphene material: 1616 and 3414 cm^{-1} , which indicated that PDA aromatic rings had an affinity to the structure of graphene, and that there was, on the graphene surface, an acid group which was small. Furthermore, intense absorption features of PDA were mainly demonstrated by the obtained PDA@graphene.

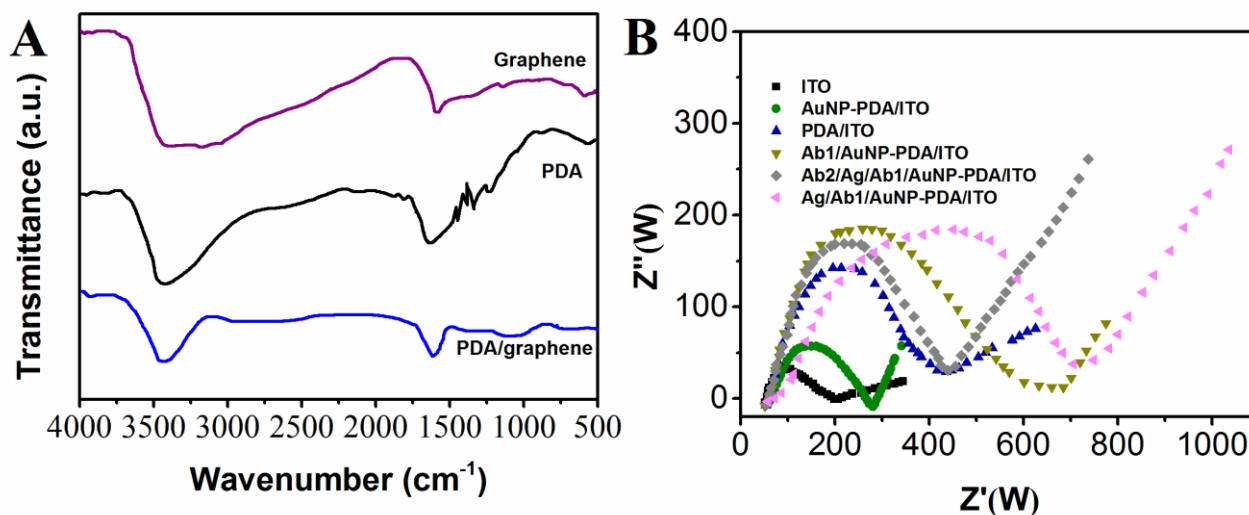


Figure 1. (A) Graphene, FTIR spectra of PDA, and PDA@graphene, (B) the EIS outcomes of the ITO, Ab₁/AuNP-PDA/ITO, AuNP-PDA/ITO, Ag/Ab₁/AuNP-PDA/ITO, PDA/ITO, AuNP-PDA@graphene-HRP-Ab₂/Ag/Ab₁/AuNP-PDA/ITO in 5.0 mM Fe(CN)₆^{3-/4-} containing 0.10 M KCl solution, respectively.

As an appropriate method to supervise the surface features, impedance spectroscopy helped make chemical processes and transformation in relation to the conductive electrode surface well-understood. A linear portion and a semicircular portion were included in the impedance spectra, and the linear portion, lower in frequencies, was in accordance with the diffusion process while the semicircle part, higher in frequencies, was in accordance with the limited process of electron-transfer, The semicircle diameter was corresponding to the electrontransfer resistance (R_{et}). Figure 1B was compared with the EIS obtained for K₃Fe(CN)₆ at the ITO, PDA/ITO, Ab₁/AuNP-PDA/ITO,

Ag/Ab₁/AuNP-PDA/ITO, AuNP-PDA/ITO, and AuNP-PDA@graphene-HRP-Ab₂/Ag/Ab₁/AuNP-PDA/ITO. An electron-transfer resistance, which was 107 Ω more or less, was demonstrated by the redox process of the [Fe(CN)₆]^{3-/4-} probe at the bare ITO electrode, and as PDA came into being on the ITO surface, this value prominently increased and reached to 344 Ω .

Nevertheless, then the Ret reduced to 263 Ω as the AuNP aggregated onto the PDA, suggesting that AuNP was a prominent electric conductor making material conducted and **accelerating** the electron transfer. Additionally, after incubation of Ab₁, the value increased to 437 Ω , which indicated that Ab₁ molecules discouraged the exchange of electrons between redox probe and the electrode, and were immobilized on the electrode. Next, the resistance was increased again under the influence of the particular interaction of Ag and Ab₁. Finally, the resistance intriguingly reduced to 446 Ω after the interaction between HRP-labeled Ab₂ and Ag. Accordingly what we suggested was that, despite that the electron transfer might be impeded by the protein adsorption in general, the AuNP-PDA@graphene, that might enhance the electron transfer due to its excellent electrochemical conductivity of graphene and AuNP, carried Ab₂ in this experiment.

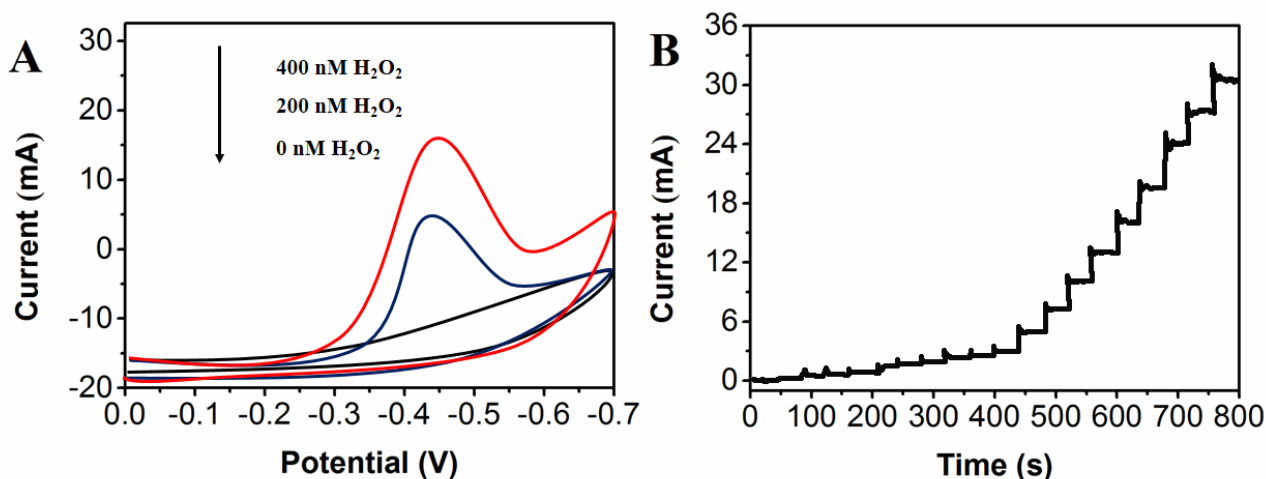


Figure 2. (A) Cyclic voltammograms in PBS (pH 7) with 0, 200, and 400 nM H₂O₂ for AuNP-PDA/ITO Scan rate: 100 mV/s. (B) Catalytic electrochemical decrease of hydrogen peroxide on AuNP-PDA/ITO at -0.46 V at different concentrations.

Experiments of bioelectronic quality control for the nanostructured electrodes were studied in this work via attaching horseradish peroxidase (HRP) onto the AuNP-PDA layer. For the immobilization of HRP, 20 μ L of 3.0 mg/mL HRP in PBS was put onto the AuNP-PDA/ITO electrode, and cleaned by water after 12 h of reaction, we use these HRP-AuNP-PDA electrodes to survey the limit and sensitivity of detection for the electrochemical determination of H₂O₂. Addition of H₂O₂ to HRP converts the iron heme peroxidase enzyme to a ferryl-oxo species that can be electrochemically reduced directly by the electrode. Using the method of amperometry, with the increase of H₂O₂ concentrations, at a utilized potential of -0.46 V vs SCE, there appeared an enhanced steady-state current (Figure 2A). By injecting a quite small amount of H₂O₂ until it was 3 times of the average noise reached by a steady-state current, a detection limit of 5.0 nM H₂O₂ was measured (Figure 2B). The sensitive detection of H₂O₂ based on AuNP-PDA shows that the AuNP-PDA platform has high

conductivity and large surface areas and can retain the activity of the biomolecule, which allows simple and stable bioconjugation to large amounts of primary antibodies [25, 26].

With the assistance of the electron mediator OPD, the immobilized HRP on the AuNP-PDA@graphene toward the decrease of H_2O_2 , is the basis of the electrochemical detection. These two sets of biocomposites, in the presence of the analyte (Ki67 antigen), respectively grounded on AuNP-PDA and AuNP-PDA@graphene, formed an immunocomplex which is of sandwich-type and the immunocomplex increases, with the increment of the Ki67 concentration in the sample. As demonstrated in Figure 3A, only weak redox peaks were showed by the CV of AuNP-PDA/ITO and HRP-anti-Ki67-AuNP-PDA@graphene complexes as the addition of 2.0 mM OPD to PBS. In correspondence to the oxidation of 2,2'-diaminoazobenzene, the enzymatic product, the CV of HRP-anti-Ki67-AuNP-PDA@graphene complexes demonstrated an oxidation peak at 0.45 V when we added 2.0 mM OPD and 4.0 mM H_2O_2 to PBS. Thus, the oxidation of OPD by H_2O_2 quickly went to completion under the catalysis of HRP. Here, the HRP carried by AuNP-PDA@graphene retained high enzymatic catalytic activity [27, 28].

A research for comparison of the amperometric responses of immunoreaction was implemented. As indicated in Figure 3B, the use of HRP and AuNP-PDA@graphene demonstrated amperometric change at a higher degree than that obtained through the other label methods. These observations might be contributed to by some possible causes. First, the immobilization density of HRP-anti-Ki67 bound might be dramatically enhanced by the high surface-to-volume ratio of bionanocomposites. Second, AuNP and graphene were doped into the bionanocomposites with electronic transfer of higher capability, which might efficiently transmit electrons from the surface of the base electrode to the HRP redox center. Third, PDA may make more graphene and AuNP attach, resulting in more HRP loading effectively to amplify the amperometric signal output. The enzyme loading is defined as the difference in the amount of the enzyme between the total enzyme used and the residual enzyme present in the supernatant after immobilization [29].

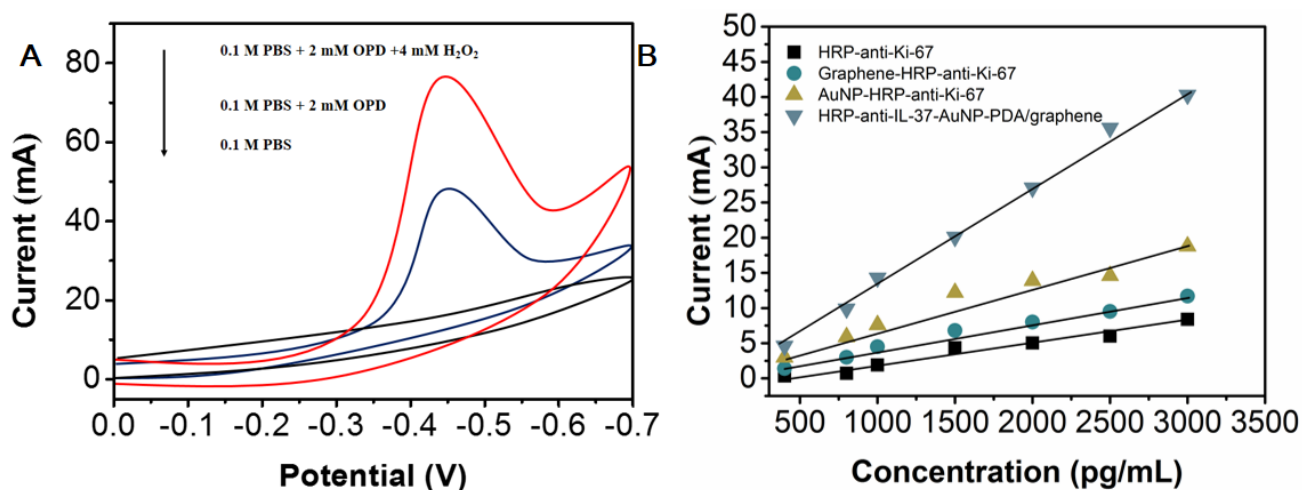


Figure 3. (A) Cyclic voltammograms of HRP-anti-Ki67-AuNP-PDA@graphene in 0.10 M pH 7 PBS, in 0.10 M pH 7.0 PBS contained 2.0 mM OPD and in 0.10 M pH 7 PBS contained 2.0 mM OPD and 4.0 mM H_2O_2 . (B) Amperometric responses of the immunosensor with the variously secondary-labeled antibody toward different Ki67 concentrations.

In order to evaluate the sensitivity and the quantitative range of the devised immunoassay, the sandwich immunoassay format was adopted to detect H_2O_2 as substrate of enzyme with OPD as the mediator under conditions that was optimized and Ki67 with AuNP-PDA@graphene labeled HRP-anti-Ki67 molecules as the tracer. Figure 4A demonstrated that, with the addition of H_2O_2 , the amperometric current from the sensor reached a steady-state response quickly, and increased in accordance with Ki67 concentration between 4.0 and 800 pg/mL, and the detection limit was 1.7 pg/mL ($S/N = 3$). The reason for the low detection limit was that the access chance of the antigen–antibody interaction could be enhanced by a large number of HRP-anti-Ki67 molecules conjugated onto the AuNP-PDA@graphene, especially as the analyte (antigen) concentration in the sample was too low. Additionally, a stable matrix was provided by PDA, which was the sensing platform. For the adsorption of AuNP, meanwhile, PDA made the sensitivity of the immunosensor improved, and more Ab_1 molecules facilitated for adsorption on the surface, and enhanced the immobilized amount of AuNP. Furthermore, from Figure 4B, the linear regression reaction could be obtained by us, which was $I(\mu A) = 1.477 + 0.1266c$ (pg/mL). The sensitivity of the HRP-anti-Ki67-AuNP-PDA@graphene was compared with that of other reported modified electrodes and the results were presented in Table 1.

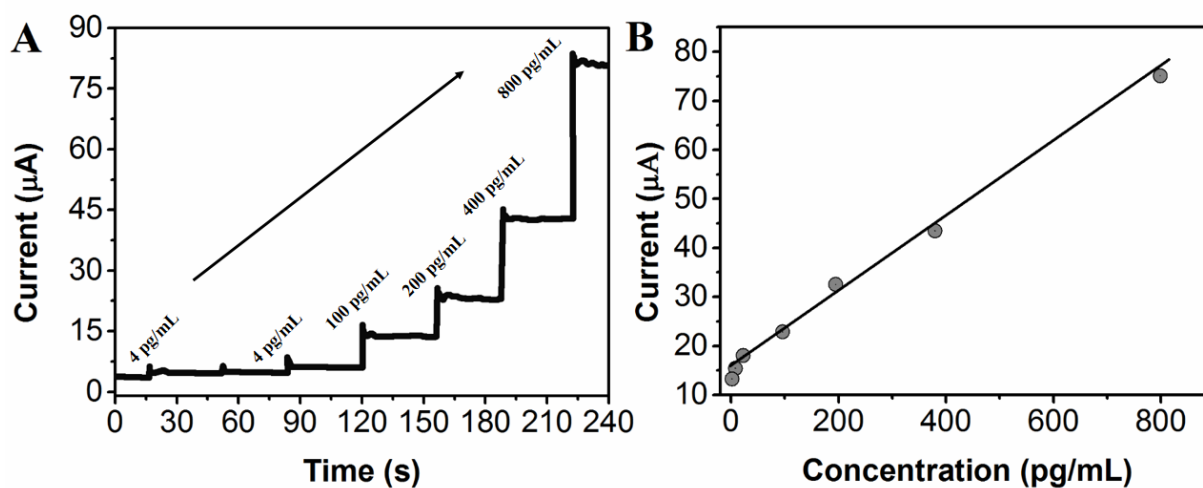


Figure 4. Amperometric results for the immunosensors incubated with different concentrations of Ki67: (A) steady-state amperometric current at -0.6 V in pH 7 PBS. (B) Immunosensor calibration plot for Ki67 ($n = 3$).

Table 1. Comparison of the present HRP-anti-Ki67-AuNP-PDA@graphene with other Ki67 determination methods.

Electrode	Linear detection range	Detection limit	Reference
Flow cytometric evaluation	5 to 100 pg/mL	3.3 pg/mL	[30]
Immunohistochemical Determination	50 to 270 pg/mL	29 pg/mL	[31]
Flow cytometry	10 to 100 pg/mL	4 pg/mL	[32]
HRP-anti-Ki67-AuNP-PDA@graphene	4 to 800 pg/mL	1.7 pg/mL	This work

Table 2. Determination of Ki67 in clinical serum samples.

Sample	Immunosensor (pg/mL)	Immunohistochemical staining (pg/mL)	RSD (%)
1	73.3	75.1	3.67
2	151.2	149.7	5.51
3	202.9	207.4	0.85
4	304.3	297.6	1.22
5	501.1	519.9	1.29

For further validation of the developed immunoassay, eight rabbit tumor model samples were analyzed utilizing the conventional immunohistochemical staining method and the proposed immunosensor. The result was demonstrated in Table 2. The relevant faults were less than 2.51%, manifesting an agreement that was acceptable between the two approaches, i.e., in the clinical laboratory, a fascinating alternative tool for PNET diagnosis might be provided by the developed immunoassay.

4. CONCLUSIONS

In this paper, we illustrated an immunosensor with strategy of amplification collaborating with HRP-anti-Ki67-AuNP-PDA@graphene probe and the AuNP-PDA platform, by using a “sandwich-assay” that is conventional. AuNP-PDA, as an effective and useful film of biointerface possessing the property of biocompatibility, expands the particular surface area of the sensing interface, and improves conductivity, contributing to the enhancement of immobilizing Ab₁ more efficiently. The method proposed could detect Ki67 concentration between 4.0 to 800 pg/mL with a limit of detection of 1.7 pg/mL ($S/N = 3$). Observing this strategy can improve the sensitivity of immunoassay, prolong the human lifetime, and consequently, provide a new promising platform for clinical immunoassay.

ACKNOWLEDGEMENT

This work was supported by Funded research projects of Qiqihar Medical University (QY2016M-06), Heilongjiang Youth Science and Technology Research Project of Traditional Chinese Medicine (ZQG-077), College Students’ Innovative Entrepreneurial Training Project in Heilongjiang Province (201611230004).

References

1. V. Adsay, *The American journal of surgical pathology*, 36 (2012) 1743.
2. C. Capella, P.U. Heitz, H. Höfler, E. Solcia and G. Klöppel, *Virchows Archiv*, 425 (1995) 547.
3. L. Zhang, C.M. Lohse, L.N. Dao and T.C. Smyrk, *Human pathology*, 42 (2011) 324.
4. G. Rindi, W.W. de Herder, D. O’Toole and B. Wiedenmann, *Neuroendocrinology*, 84 (2007) 155.
5. T. Yamaguchi, T. Fujimori, S. Tomita, K. Ichikawa, H. Mitomi, K. Ohno, Y. Shida and H. Kato, *Diagnostic pathology*, 8 (2013) 1.
6. D.S. Klimstra, I.R. Modlin, N.V. Adsay, R. Chetty, V. Deshpande, M. Gönen, R.T. Jensen, M. Kidd, M.H. Kulke and R.V. Lloyd, *The American journal of surgical pathology*, 34 (2010) 300.

7. G. Rindi, G. Klöppel, H. Alhman, M. Caplin, A. Couvelard, W. De Herder, B. Eriksson, A. Falchetti, M. Falconi and P. Komminoth, *Virchows Archiv*, 449 (2006) 395.
8. M.D. Reid, P. Bagci, N. Ohike, B. Saka, I.E. Seven, N. Dursun, S. Balci, H. Gucer, K.-T. Jang and T. Tajiri, *Modern Pathology*, 28 (2015) 686.
9. E. Fitzer, K.-H. Kochling, H. Boehm and H. Marsh, *Pure and Applied Chemistry*, 67 (1995) 473.
10. J.S. Bunch, A.M. Van Der Zande, S.S. Verbridge, I.W. Frank, D.M. Tanenbaum, J.M. Parpia, H.G. Craighead and P.L. McEuen, *Science*, 315 (2007) 490.
11. Y. Shi, K.K. Kim, A. Reina, M. Hofmann, L.-J. Li and J. Kong, *ACS nano*, 4 (2010) 2689.
12. J. Narang, N. Malhotra, C. Singhal, A. Mathur, D. Chakraborty, A. Anil, A. Ingle and C.S. Pundir, *Biosensors and Bioelectronics*, 88 (2017) 249.
13. E. Asadian, S. Shahrokhian, A.I. Zad and F. Ghorbani-Bidkorbeh, *Sensors and Actuators B: Chemical*, 239 (2017) 617.
14. R. Sivasubramanian and P. Biji, *Materials Science and Engineering: B*, 210 (2016) 10.
15. S.H. Kim, J.A. Kaplan, Y. Sun, A. Shieh, H.L. Sun, C.M. Croce, M.W. Grinstaff and J.R. Parquette, *Chemistry—A European Journal*, 21 (2015) 101.
16. S.H. Kim, Y. Sun, J.A. Kaplan, M.W. Grinstaff and J.R. Parquette, *New J Chem*, 39 (2015) 3225.
17. F. Liu, Y. Sun, C. Kang and H. Zhu, *Nano LIFE*, 6 (2016) 1642002.
18. Y. Li, M. Liu, C. Xiang, Q. Xie and S. Yao, *Thin Solid Films*, 497 (2006) 270.
19. Y. Fu, P. Li, L. Bu, T. Wang, Q. Xie, X. Xu, L. Lei, C. Zou and S. Yao, *J Phys Chem C*, 114 (2010) 1472.
20. S.-J. Li, L.-L. Hou, M.-Z. Chang, J.-J. Yan and L. Liu, *Int. J. Electrochem. Sc.*, 11 (2016) 2887.
21. Y. Wang, Y. Xiong, J. Qu, J. Qu and S. Li, *Sensors and Actuators B: Chemical*, 223 (2016) 501.
22. J. Zhang, H. Yang, G. Shen, P. Cheng, J. Zhang and S. Guo, *Chemical Communications*, 46 (2010) 1112.
23. M. Ahmad, E. Ahmed, Z.L. Hong, J.F. Xu, N.R. Khalid, A. Elhissi and W. Ahmed, *Appl. Surf. Sci.*, 274 (2013) 273.
24. X. Li, Q. Wang, Y. Zhao, W. Wu, J. Chen and H. Meng, *Journal of colloid and interface science*, 411 (2013) 69.
25. R. Li, F. Feng, Z.-Z. Chen, Y.-F. Bai, F.-F. Guo, F.-Y. Wu and G. Zhou, *Talanta*, 140 (2015) 143.
26. D. Wang, Y. Zheng, Y. Chai, Y. Yuan and R. Yuan, *Chemical Communications*, 51 (2015) 10521.
27. J. Guo, X. Han, J. Wang, J. Zhao, Z. Guo and Y. Zhang, *Analytical biochemistry*, 491 (2015) 58.
28. K. Chan, H. Lim, N. Shams, S. Jayabal, A. Pandikumar and N. Huang, *Materials Science and Engineering: C*, 58 (2016) 666.
29. S. Van Der Heide and D.A. Russell, *Journal of colloid and interface science*, 471 (2016) 127.
30. A. Poggi, B. Miniscalco, E. Morello, S. Comazzi, M. Gelain, L. Aresu and F. Riondato, *Veterinary and comparative oncology*, 13 (2015) 475.
31. I.K. Stromar and J. Jakic-Razumovic, *Applied Immunohistochemistry & Molecular Morphology*, 22 (2014) 524.
32. Y. Sun, K. Yang, T. Bridal and A.G. Ehrhardt, *Future Science*, 8 (2016) 2399.